Journal of Computational Physics **173,** 175–186 (2001)
doi:10.1006/jcph.2001.6870, available online at http://www.idealibrary.com on IDEAL®

Photon Transport through Plasmas with Density and Velocity Structure

Jason Cullen

Research Centre for Theoretical Astrophysics and Department of Theoretical Physics, University of Sydney, Sydney, NSW 2006, Australia
E-mail: cullen@physics.usyd.edu.au

Received December 1, 2000; revised May 25, 2001

The problem of inverse Compton scattering (ICS) of photons and electrons in plasmas is of importance for high-energy astrophysics. One example is the scattering of photons in an accretion flow. However, most Monte Carlo codes used in this field are not capable of investigating scattering in plasmas with smooth temperature and density gradients, and treating bulk motion is difficult even for simple cases. With the introduction into the field of algorithms associated with nonlinear Monte Carlo codes, these problems are now tractable numerically. Nonlinear Monte Carlo codes can already handle arbitrary velocity structures in a plasma. Here an extension of the algorithm is proposed that enables the calculation of scattering in plasmas with nonconstant density as well as nonconstant temperature and/or bulk motion. Scattering at low optical depths also can be studied. A code using this method can study the ICS problem in a wide variety of accretion flows, and do so exactly.

1. INTRODUCTION

The inverse Compton scattering (ICS) process is important in high-energy astrophysics. Many astrophysical systems such as x-ray binaries and active galactic nuclei produce photon spectra in the x-ray energy band. These x-ray photons are thought to be produced when a low-energy photon enters a region of hot plasma and scatters off relativistic electrons. The photon gains some energy from the electrons at each scattering event by ICS, and before escaping from the plasma the photon has typically been scattered up to x-ray energies, or even gamma-ray energies. Thus we are interested in the transport of photons through a plasma as they gain energy at a succession of scattering events. Spectra given by this process are said to be "Comptonized."

Analytic approaches to the problem generally assume the diffusion approximation for the transport as well as diffusion in energy space. The energy diffusion assumption does not hold in most plasmas of astrophysical interest because a photon's energy changes by a large

0021-9991/01 $35.00

amount at a scattering event. In rarefied plasmas, the distance between scattering events can be large, and so the spatial diffusion approximation also is a poor one. In addition, the mean free path of the photons is a function of the photons' energy as well as the plasma density, which complicates the spatial transport. The entire situation is further complicated if the geometry of the plasma is not trivial, if other processes (such as absorption) are taken into account, and if complicated photon source functions are to be investigated. Spectra that are formed by this process are therefore often calculated using Monte Carlo techniques. An added advantage of using Monte Carlo simulations is their flexibility: these codes can be modified easily to be applicable to many areas of interest in high-energy astrophysics.

The most common Monte Carlo simulations in this branch of astrophysics are analogue simulations [1]. A photon of some energy is injected into the plasma, an integral is performed to determine the mean free path, and the location of the next scattering point is found. At this point, the scattering event is modeled by sampling the differential cross section, and the new energy and new direction is assigned to the photon. The photon is followed until it escapes the plasma. After following many photons, a spectrum is built up. An importance sampling technique is sometimes used to treat the spatial transport, whereby a weighted fraction of the photon is forced to scatter, while the rest of the photon escapes. The weight function is determined at each scattering point by the probability of escape from the plasma [2]. This is useful when the probability of a given photon undergoing a scattering event is very small.

These codes have been used to treat the Comptonization problem in regions where the plasma has a well-defined temperature and a homogeneous density. However, astrophysical plasmas are unlikely to be homogeneous and isothermal. Additionally, treating builk motion of the plasma with such a code is difficult even for simple cases.

By dividing the plasma into various zones, with each zone having a different temperature and density, density and temperature variations can be studied in a crude way, e.g., by having the density decrease in a series of steps. An improvement on this situation was made by Hua [3], who developed a code to treat smooth density variations, but the plasma was still required to be isothermal, and no bulk motion was considered.

The current state of the art for the Comptonization problem is the nonlinear Monte Carlo (NLMC) code introduced into the field by Stern *et al*. [4]. This method uses a von Neumann rejection algorithm for finding the location of the next scattering point. This has numerous advantages, as will be described.

In Section 2 we review for completeness the currently used methods of photon transport. In Section 3 we propose a method of combining the Hua and Stern algorithms that enables the treatment of smooth density variations in the presence of temperature variations and bulk motion. In Sections 4 and 5 we discuss implementation and give examples of astrophysics problems that now can be tackled with such a code.

Detailed discussions of how to model the actual scattering events were given by Hua [3], Gorecki and Wilczewski [5], and especially Pozdnyakov *et al*. [1], and so will not be discussed here.

2. PHOTON TRANSPORT

In following a photon through the simulation, one must find where the next scattering point will be. Typically in a linear simulation, the distance l to the next scattering point is

determined by inverting the cumulative probability distribution

$$\xi = e^{-\tau} \equiv e^{-\int_0^l n(s)\sigma ds}, \tag{1}$$

where τ is called the optical depth, ξ is a uniform random number between zero and one, and the cross section σ has been averaged over the distribution of target electrons. $n(s)$ is the electron density along the photon's path s. For a constant density $n(s) = n$, we therefore have the expression

$$l = -\frac{1}{n\sigma} \ln(\xi). \tag{2}$$

2.1. Current NLMC Method

Nonlinear Monte Carlo codes take a somewhat different approach to solving the transport problem. The rate of scattering events for a beam of photons (where the beam consists of a single photon, say) incident with a beam of electrons at some point is

$$n\sigma_{\mathrm{KN}} V_{\mathrm{rel}}. \tag{3}$$

This quantity is used to determine if a scattering event takes place. It depends on the photon's energy through the Klein–Nishina cross section for electron–photon scattering, σ_{KN}, and the temperature of the electrons through the relative velocity V_{rel} (because the temperature determines how fast our target electron is moving and hence the relative velocity between the photon and the electron).

The interaction rate is used if we are interested in the time between scattering events rather than the distance (2). We then have the expression

$$t = -\frac{1}{n\sigma_{\mathrm{KN}} V_{\mathrm{rel}}} \ln(\xi), \tag{4}$$

where $n\sigma V_{\mathrm{rel}}$ is the rate of scattering events and it has been assumed that all the electrons have the same V_{rel}.

This is, of course, not a realistic assumption. Each electron has a different velocity V_{rel} relative to the photon. The real interaction rate (which for a complicated situation is difficult to evaluate) is the sum of all the partial interaction rates of all the electrons in the plasma! We do not wish to sum over all the electrons in the simulation, so the algorithm used by nonlinear codes assumes the existence of a virtual process, such that [4]

$$n(\sigma_{\mathrm{KN}} + \sigma_{\mathrm{virt}}) V_{\mathrm{rel}} \equiv n\sigma_{\mathrm{T}} \cdot 2c, \tag{5}$$

where σ_{T} is the Thompson cross section, σ_{KN} is the Klein–Nishina cross section, and c is the speed of light. Because one is often interested in scattering in regions of homogeneous density, n is dropped from the above to give

$$(\sigma_{\mathrm{KN}} + \sigma_{\mathrm{virt}}) V_{\mathrm{rel}} = \sigma_{\mathrm{T}} \cdot 2c. \tag{6}$$

It is possible for V_{rel} to be greater than c for some collisions; e.g., the relative velocity of the photon with respect to the electron is given in Ref. [6] as $\mathbf{c} - \mathbf{v_e}$, where $\mathbf{c}$ is the

photon velocity vector and $\mathbf{v}_e$ is electron velocity vector, assuming collinear vectors. This can approach $2c$ and hence explains the factor of $2c$ in Eq. (5).

The use of a virtual process is known in the nuclear engineering literature as "delta scattering," "fictitious forward scattering," or "Woodcock tracking" and was first used in [7]. The technique also is used for transporting electrons in the electron gamma show code [8]. The purpose of introducing the virtual process is that the right-hand side of Eq. (5) is an upper limit on the real interaction rate and is constant, so it is easy to use this value to determine the time to the next interaction event. In fact, we have

$$t = -\frac{1}{n\sigma_T \cdot 2c} \ln(\xi). \tag{7}$$

We then find/choose an electron for the photon to scatter with. But having used the right-hand side of (5), we have to disregard the virtual (unphysical) process and determine if a real scattering event takes place. To put it another way, the probability of an interaction is the sum of the probability of the virtual process occurring and the probability of the real process occurring. Therefore, the real scattering event is accepted/selected with a probability

$$\frac{\sigma_{KN} V_{rel}}{\sigma_T \cdot 2c}; \tag{8}$$

otherwise the event is rejected as being due to the virtual process, and the photon continues without scattering until the next time step.

This rejection algorithm is efficient except if the electron is moving relativistically in the same direction as the photon, in which case V_{rel} becomes small, and if the photon energy is very large, in which case the cross section σ_{KN} becomes small.

The benefits of such a procedure are:

- it can be extended easily to include other processes;
- no integrals for determining the mean free path through the electrons are required; and
- finding a tentative scattering point does not require any knowledge of the velocity structure in the accretion flow, so this algorithm can easily handle problems where there is bulk motion of the flow, as expected for accretion problems. This was a huge advance on "linear" codes, which are generally used to consider isothermal flows without bulk motion.

To use such a method to treat bulk motion of the flow, we simply determine a (potential) scattering point using $n\sigma_T \cdot 2c$ as the rate of scattering events (Eq. (7)). We then ask, "What is the direction and momentum of the accretion flow at this tentative point?" This gives us the relative velocity of the electron that we need for the rejection test. We then calculate the real cross section and accept or reject the scattering event using Eq. (8). If the event is rejected, the photon continues on its way until the next time step. Or if we are studying an accretion flow with a temperature gradient, at the tentative scattering point we ask what the temperature is at this point, draw an electron from a distribution with this temperature, and then decide to accept or reject the scattering event.

3. PROPOSED EXTENSION OF THE ALGORITHM

Hua *et al*. [3] described how a nonconstant density profile can be integrated over to find the next scattering point using an expression equivalent to Eq. (1). They have implemented

this method for an isothermal plasma with an r^{-1} and $r^{3/2}$ density profile using a linear code.

Here we include this idea in the NLMC method and propose that instead of finding the next scattering point using $n\sigma_T \cdot 2c$, we find the scattering location by integrating over a nonconstant density profile. The interaction rate is now given by

$$n(s) \cdot \sigma_T \cdot 2c, \tag{9}$$

where $n(s)$ is the density along a photon path parameterized by s.

If one is interested in sampling the time between scattering events for the case where the density along the photon trajectory is not constant, instead of Eq. (1) we have the integral

$$\xi = e^{-\int_0^{2ct} n(s)\,\sigma_T\,ds} \tag{10}$$

or rearranging,

$$\int_0^{2ct} n(s)\sigma_T\,ds = -\ln(\xi). \tag{11}$$

If $n(s)$ is constant, then the above reduces to Eq. (7). The factor of $2c$ in the upper limit of the integral is required because we are interested in scattering events in which the rate of scattering is given by Eq. (9). The distance to the next scattering point is then just the time multiplied by the speed of light.

The distance above can be thought of as a lower limit on how far the photon really travels because it uses an upper limit on the interaction rate. In reality the cross section is not σ_T and the relative velocity is not $2c$. So this scattering point is only "tentative."

Having found a tentative interaction point, the real interaction rate at the scattering point plus the virtual interaction rate is taken to be

$$n(s)(\sigma_{KN} + \sigma_{virt})V_{rel} \equiv n(s)\sigma_T \cdot 2c. \tag{12}$$

So we accept the tentative scattering event with probability

$$\frac{n(s)\sigma_{KN}V_{rel}}{n(s)\sigma_T \cdot 2c} = \frac{\sigma_{KN}V_{rel}}{\sigma_T \cdot 2c}. \tag{13}$$

This procedure is completely analogous to the previous section. The only difference to the algorithm is that we are performing the distance integral explicitly rather than using an expression that can be integrated in closed form and inverted. This procedure is relativistic and exact: no approximations have been made.

4. DISCUSSION

The efficiency of accepting a scattering event is independent of the density at that point because $n(s)$ has canceled in Eq. (13). The integration over the density profile is now the most time-intensive part of the code. This modified algorithm still can be used if photons are weighted in energy. (In fact this is required for good spectral resolution [4].) Once a scattering point is accepted we evaluate the velocity profile or temperature profile to give

us the properties required for the electron the photon will scatter with. It is not necessary to search through some array of electrons because electrons are not followed in the simulation. The velocity or temperature profiles (specified beforehand) give all the information about the electrons at the scattering point. This increases the speed of the code but also means the code cannot treat processes in which electrons must be followed (i.e., pair annihilation). The main advantage is that arbitrary density and temperature gradients, with or without bulk motion, can be considered without recourse to zones. Furthermore, this can be done while retaining all of the features that have made Monte Carlo codes popular, such as the capacity to treat complex geometries and source functions.

As for how such an algorithm may be used, we can consider bulk motion or a temperature gradient as before, but now we also can study density gradients as well. This has numerous applications in high-energy astrophysics, such as accretion columns with density, temperature and velocity structure falling onto (weakly magnetized) neutron stars, or scattering in accretion flows surrounding black holes. We can of course extend Hua's model to include temperature gradients. A mixture of thermal and bulk motion for the electrons can be studied at the tentative scattering point by first considering a frame instantaneously co-moving with the flow so that an electron can be drawn from a Maxwellian distribution and assigned a random direction of motion. Having the electrons' (thermal) properties, a Lorentz transform can be performed out of the flow frame and into the "lab" frame to obtain the "resultant" vector. This vector (momentum and direction of the electron) is then sent to the rejection algorithm (13) to determine if the interaction is accepted or not.

5. EXAMPLES

As an example of the technique, photon scattering by cold and freely falling electrons is considered. The geometry of the electron plasma is considered to be spherical, with the photon source located at the center. Two different photon source functions are considered, in particular a line at 6.4 keV and a power law extending from 2 to 100 keV, both of which are common in x-ray astrophysics. Previous treatments of this problem have had to assume a cross section constant with energy and slowly moving electrons [9].

Figure 1 shows a Comptonized line with injected energy of 6.4 keV. The solid curve is after scattering in a sphere of cold (stationary) electrons of optical depth $\tau = 3.0$, while the dashed line is for scattering in cold electrons with a radial density profile of the form

$$n(r) = (n_0)(r/R + 1)^{-3/2}, \tag{14}$$

where $n(0)$ is the density at the origin defined so that a sphere of constant density $n(0)$ would have an optical depth of 3.0. Both lines are injected at the origin (center of the sphere). Line broadening occurs as a result of electron scattering. It can be seen that in the presence of the density gradient the line is less broad because the photons have to travel through less optical depth to escape from the sphere.

Figure 2 shows the same 6.4 keV line scattering through the same density gradient but where a velocity gradient of the form

$$v(r) = (v_0)(r/R + 1)^{-1/2} \tag{15}$$

has been added. A density profile $\propto n^{-3/2}$ and a velocity profile $\propto v^{-1/2}$ are appropriate for electrons that are falling freely under gravity onto some accreting object. The solid curve

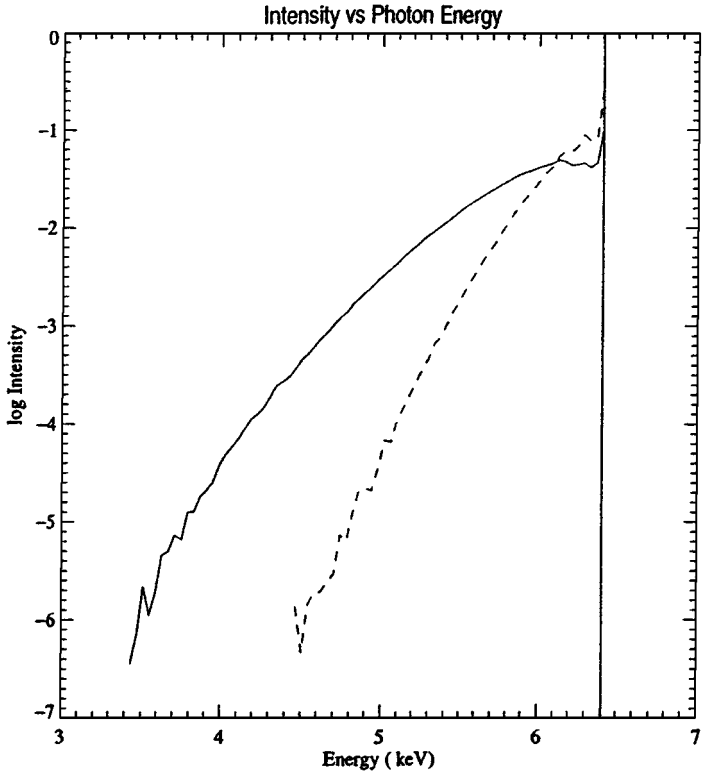

FIG. 1. Scattering of a 6.4 keV line by cold electrons.

is for $v_0/c = 0.03$, the dashed curve is for $v_0/c = 0.05$, and the dot-dashed curve is for $v_0/c = 0.07$. The slope of the high-energy wing of the line depends on v_0.

Figure 3 shows the distortion of a power law of energy index $\alpha = 1.0$ due to scattering by cold electrons in a spherical geometry. The solid curve is the injected power law, which extends from 2 to 100 keV. The power-law photons are injected at the origin of the sphere. The dashed curve is the resulting Compton scattered spectrum for a sphere of constant density and optical depth $\tau = 3.0$. The dot-dashed curve is the result of scattering by cold electrons with a density profile given by Eq. (14). The presence of the density gradient pushes up the energy at which the break in the power law occurs because there is less total optical depth from the center to the edge of the sphere so fewer scattering events take place.

Figure 4 shows the distortion of a power law of energy index $\alpha = 1.0$ due to scattering by electrons with a density profile given by Eq. (13) and a velocity profile given by Eq. (14). The dot-dot-dot-dashed, dot-dashed, short-dashed, and long-dashed curves correspond to a v_0/c of 0.1, 0.3, 0.6, and 0.8, respectively. (The long-dashed curve has been shifted downward compared with the other curves because extra energy bins were used for this case.) For low velocities the spectrum has almost the same form as for the cold-electron case. As the velocity increases, curvature is introduced into the power law; then the power law becomes flat ($\alpha \sim 1.0$). At large velocities a peak is formed above 100 keV.

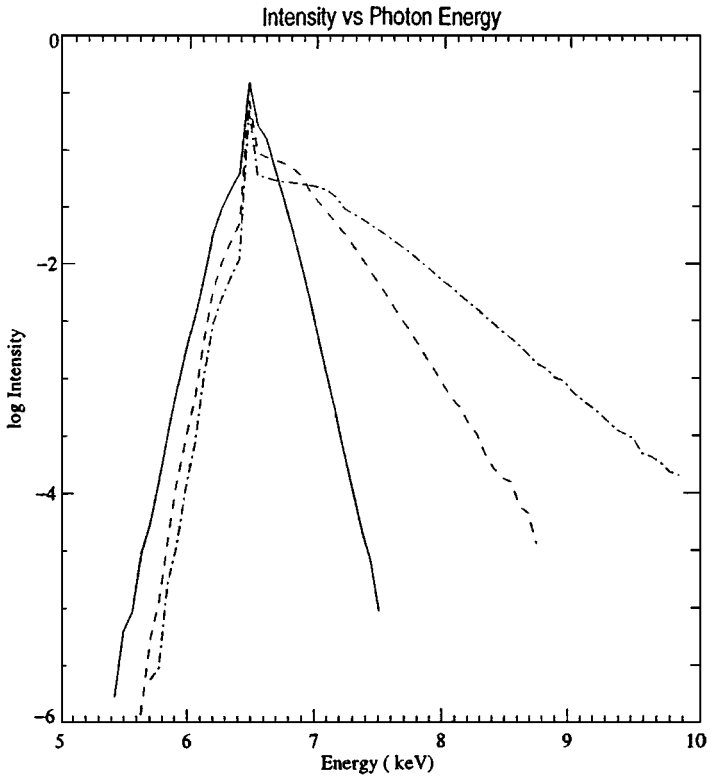

FIG. 2. Scattering of a 6.4 keV line by freely falling electrons.

5.1. Low Optical Depth

Low optical depths present a problem as many photons can be injected and then escape without scattering at all. The problem of scattering at low optical depths has therefore been treated with linear codes using a technique of forced scattering. Each simulation photon carries a number or "weight," which describes the number of "real" photons to which it corresponds. Instead of the usual method of finding the scattering point, the normalization of the cumulative distribution function is changed to force the photon to scatter in the plasma;

$$\xi = (1 - e^{-n\sigma l})/(1 - e^{-n\sigma d}), \tag{16}$$

where d is the distance to the edge of the cloud along the photon's path and $\boldsymbol{l}$ is the distance the photon travels (constant density has been assumed for this section). Inverting this for $\boldsymbol{l}$ gives

$$\boldsymbol{l} = -\frac{1}{n\sigma} \ln(1 - \xi(1 - e^{-n\sigma d})). \tag{17}$$

To make this procedure physical, the photon's weight w_{old} is then changed so that part of the weight associated with the photon escapes from the plasma and is binned. The photon (with a suitably reduced weight) continues scattering inside the cloud. The escaping weight has the value

$$w_{esc} = w_{old} e^{-n\sigma d}, \tag{18}$$

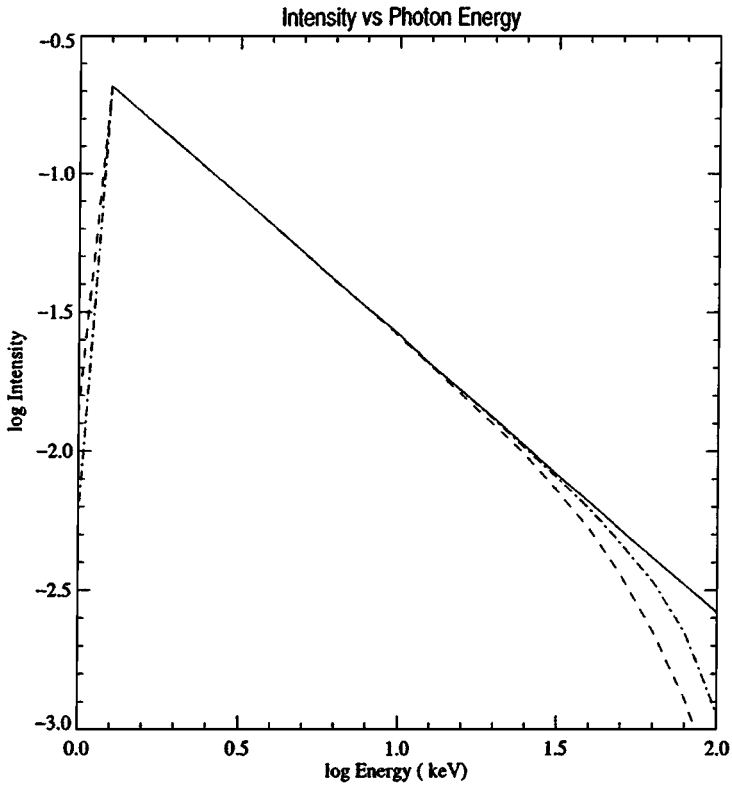

FIG. 3. Scattering of powerlaw photons by cold electrons with constant density and by electrons with a density gradient.

while the photon weight is given the new value

$$w_{new} = w_{old} - w_{esc}. \tag{19}$$

After following many photon trajectories, the escaping weights w_{esc} build up the resulting spectrum. For an example of this procedure in investigating the Sunyaev–Zeldovich effect, see Molnar and Birkinshaw [2].

This procedure can also be made to work for NLMC transport. This enables investigation of bulk-motion scattering and scattering through temperature gradients in low optical depth plasmas without making approximations.

Consider a simulation photon at some point in the plasma, and take $\sigma = \sigma T$ in the above expressions. A fraction of the weight given by Eq. (16) escapes and is binned. Equation (15) then is used to find a tentative scattering point. Note that the escaping fraction of the weight is binned whether or not the tentative scattering event is accepted. The photon then has its weight adjusted. If the scattering event is accepted, the photon changes energy and direction and the simulation proceeds. If the scattering event is rejected, the photon location is updated to the location of the tentative scattering point and another tentative scattering point is drawn without changing the photon's direction. The photon can "step" its way through the plasma with part of its weight escaping at each "step" even if it is not scattering.

This procedure has been used to produce the curves in Fig. 5. The solid curve is a blackbody spectrum injected at the origin of a sphere of constant density. The optical depth

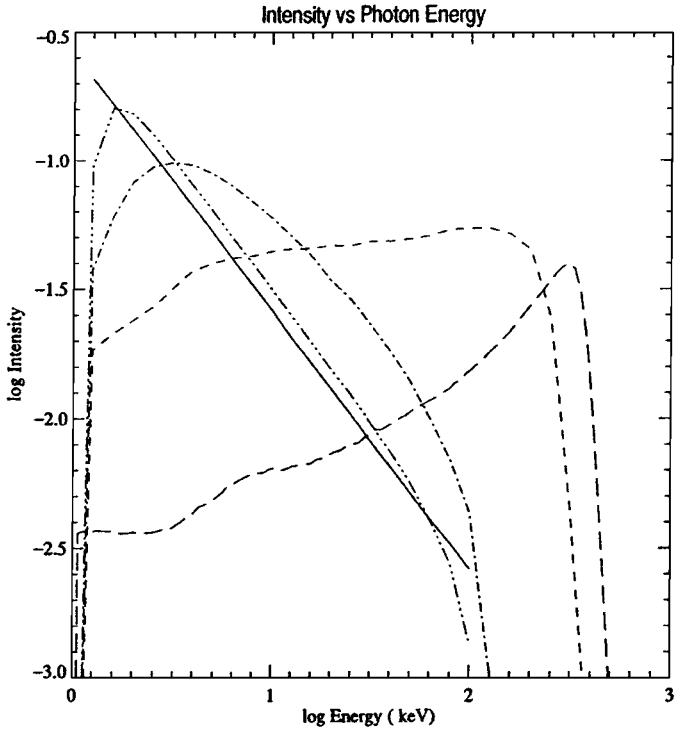

FIG. 4. Scattering of powerlaw photons by freely falling electrons.

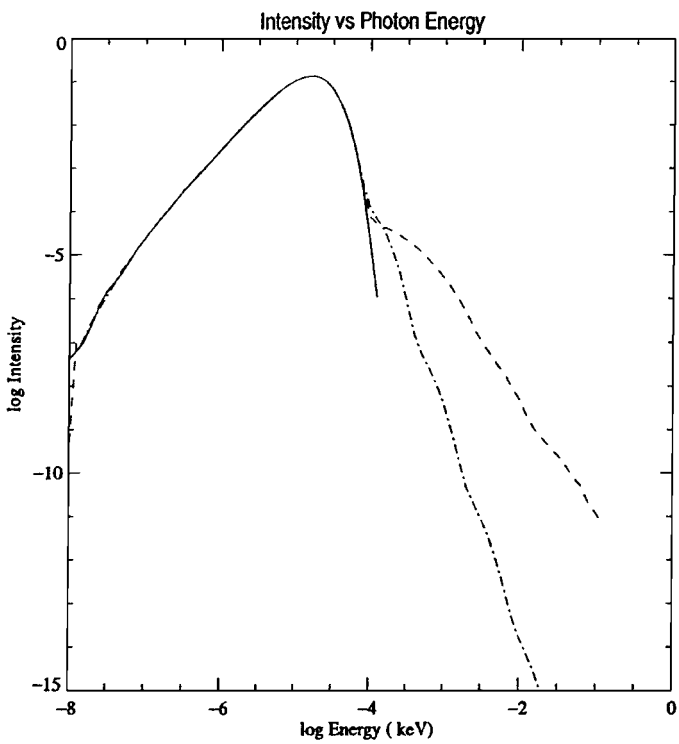

FIG. 5. Bulk-motion scattering for $\tau = 0.001$ and thermal scattering for $\tau = 0.001$, for blackbody source photons.

of the sphere is $\tau = 0.001$. The dashed line is the resulting Comptonized spectrum for an isothermal plasma of temperature 250 keV, while the dot-dashed line is produced by bulk-motion Comptonization in a converging spherical flow of constant density. The flow is directed toward the origin at the center of the sphere, and the flow velocity is constant and set equal to $v/c = 0.67$. The optical depth is again $\tau = 0.001$. Different velocity profiles and/or temperature profiles can be included as described in Section 4. This is a flexible way of treating velocity and temperature gradients in low optical depth plasmas.

6. CONCLUSION

The NLMC transport method has been extended to include density gradients. This could have various applications in astrophysics, where plasmas may not be homogeneous and isothermal. The density can be smoothly varying, and density zones are not required. The method of forced scattering has also been demonstrated to work within the framework of the NLMC method, meaning that plasmas containing temperature and velocity structure now can be considered even if the scattering plasma is of small optical depth.

One of the original reasons the NLMC codes were developed was to study the cooling of a plasma by inverse Compton scattering in a self-consistent manner. An example of such a calculation was given by Malzac and Jourdain [10], where the optical depth of a homogeneous plasma is allowed to vary until the rate of energy loss through scattering events equals the rate of energy injection in the form of new particles. In principle this is still possible for the modified algorithm considered here, if we imagine fixing the shape of the density and temperature distributions, while allowing the normalization of the density profile to move up and down. This corresponds to injecting more electrons or removing electrons until the rate energy is removed equals the rate energy is being injected (which would be calculated by integrating over the density and temperature distributions). These sorts of calculations are more demanding than pure Comptonization problems and so have not been considered here.

One restriction on the method is that it cannot study electron–positron pair cascades, because only photons are followed in the code. Other than this, it is a flexible way of treating the Comptonization problem.

APPENDIX

In the case of a photon interacting with electrons, the relativistic expression for the reaction rate is [11]

$$\sigma_{\mathrm{KN}} \frac{P_{1\mu} P_2^{\mu}}{E_1 E_2} n, \tag{A1}$$

where $P_{1\mu}$ is the momentum four-vector of particle 1 (the photon, say), P_2^{μ} is the momentum four-vector of particle 2 (target particle), E_1 and E_2 are the energies of particles 1 and 2, σ_{KN} is the cross section, and n is the density of target electrons.

The four-vector contraction is $P_{1\mu} P_2^{\mu} = E_1 E_2 - \mathbf{p_1 p_2}$, where $\mathbf{p_1}$ and $\mathbf{p_2}$ are the momentum vectors of the particles, and so

$$\frac{P_{1\mu} P_2^{\mu}}{E_1 E_2} = \frac{E_1 E_2 - \mathbf{p_1 p_2}}{E_1 E_2} = \left(1 - \frac{\mathbf{p_1}}{E_1} \cdot \frac{\mathbf{p_2}}{E_2}\right) = (1 - \mathbf{\Omega} \cdot \mathbf{v}), \tag{A2}$$

where $\mathbf{\Omega}$ is the unit vector in the photon propagation direction and $\mathbf{v}$ is the electron velocity vector, and with units where $c \equiv 1$ being assumed. On comparison of Eq. (A1) with Eq. (3) one sees that correct reaction rates are obtained if the quantity $(1 - \mathbf{\Omega} \cdot \mathbf{v})$ is identified with $V_{\rm rel}$ as used in this paper.

REFERENCES

1. L. A. Pozdnyakov, I. M. Sobol, and R. A. Sunyaev, Comptonization and the shaping of X-ray source spectra: Monte Carlo calculations, *Astrophys. Space Sci.* **2**, 189 (1983).
2. S. M. Molnar and M. Birkinshaw, Inverse Compton scattering in mildly relativistic plasma, *Astrophys. J.* **523**, 78 (1999), arXiv:astro-ph/9903444.
3. X. Hua, Monte Carlo simulation of Comptonization in inhomogeneous media, *J. Comput. Phys.* **11**, 660 (1997), arXiv:physics/9709023.
4. B. Stern, M. Begelman, M. Sikora, and R. Svensson, A large particle Monte Carlo code for simulating non-linear high-energy processes near compact objects, *Mon. Not. R. Astron. Soc.* **272**, 291 (1995).
5. A. Gorecki and W. Wilczewski, A study of Comptonization of radiation in an electron plasma using the Monte Carlo method, *Acta Astron.* **34**, 141 (1984).
6. W. Greiner and J. Reinhardt, *Quantum Electrodynamics*, 2nd ed. (Springer-Verlag, Berlin/New York, 1996), p. 176.
7. Woodcock *et al.*, Techniques used in the GEM code for Monte Carlo neutronics calculations in reactors and other systems of complex geometry, in *Proceedings of the Conference on the Application of Computing Methods to Reactor Problems*, ANL-7050 (Argone National Lab, May 1965).
8. W. R. Nelson, H. Hirayama, and D. W. O. Rogers, The EGS code system, SLAC Report 266. Section 2.4 (particle transport) (Stanford Linear Accelerator Center, 1985). See also http://ehssun.lbl.gov/egs/egs.html.
9. M. Colpi, Multiple Compton scattering by thermal electrons in a spherical inflow: The effects of bulk motion, *Astrophys. J.* **326**, 223 (1988).
10. J. Malzac and E. Jourdian, IC emission above a disk, in *Proceedings of Third INTEGRAL Workshop*, Astrophysical Letters and Communications **38**, (1999), arXiv:astro-ph/9901186.
11. L. D. Landau and E. M. Lifshitz, *The Classical Theory of Fields*, 3rd ed. (Pergamon, Elmsford, NY, 1971), Chapter 2, Section 12.